

Short Communication

## Corrosion Behavior of X65 and X80 Pipeline Steels under AC Interference Condition in High pH Solution

Min Zhu<sup>\*</sup>, Yongfeng Yuan, Simin Yin, Shaoyi Guo

School of Mechanical Engineering & Automation, Zhejiang Sci-Tech University, Hangzhou 310018, PR China

\*E-mail: [zmii666@126.com](mailto:zmii666@126.com)

Received: 27 July 2018 / Accepted: 20 August 2018 / Published: 1 October 2018

---

The corrosion behavior of X65 and X80 pipeline steels under AC interference in high pH solution was investigated by potentiodynamic polarization curve, open circuit potential, Mott-Schottky curve and immersion test. The results show that AC could significantly reduce the passivity of the steels, interfere with the formation of passive film, increase the instability of passive film formed on the steel, and AC with high  $i_{AC}$  generates a more damage to the film. The film on X65 steel has a worse stability, with a larger corrosion rate. Under AC interference, X65 steel has a worse corrosion resistance, with a more severe localized corrosion. While X80 steel exhibits a better corrosion resistance, with a slighter corrosion status. The microstructure consisting of ferrite and pearlite is more susceptibility to AC corrosion.

---

**Keywords:** AC interference; passive film; stability; corrosion resistance; microstructure

### 1. INTRODUCTION

With rapid development of electricity, energy and transportation industry, the increasing buried steel pipelines are installed in proximity to overhead high-voltage AC power transmission lines or AC-powered rail transit systems due to the limited spaces to install these facilities. In this case, AC induced corrosion is becoming the huge threat to the safe operation of buried pipelines[1-4]. Some research found that AC interference could improve the corrosion rate of pipeline steel [5-7]. Xu [8] indicated that the corrosion of 16Mn pipeline steel was accelerated by the applied AC current density of 0-400A/m<sup>2</sup>. Fu [9] reported that uniform corrosion occurred on the steel at a low AC current density, while severe pitting corrosion was observed under a high AC current density. Song [10] thought that the corrosion rate of steel can be affected by AC voltage, AC current density and AC frequency. Kuang [11] demonstrated that pitting corrosion could be formed on the steel at sufficiently high AC current densities in both high pH and near-neutral pH solutions. Our previous research [12-13] indicated that

AC could increase the SCC susceptibility of X80 pipeline steel in carbonate/bicarbonate solution, and some cracks were found to have initiated from the pits induced by AC. Wang and Wan[14-15] also demonstrated that superimposed AC could enhance the SCC susceptibility of pipeline steel, which was attributed to the influence of hydrogen embrittlement.

At present, X80 steel as the preferred metal of oil/gas buried pipeline are widely used throughout the world due to its good comprehensive properties. With the evolution of microstructure of pipeline steel, the corrosion behavior of pipeline steels under AC interference may be different. However, by now, no relative literature has reported the relationship between AC corrosion behavior and microstructure of pipeline steel. In order to investigate this aspect, X65 pipeline steel is selected as the experimental reference material. Therefore, the corrosion behavior of X65 and X80 pipeline steels under AC interference in high pH solution was studied by potentiodynamic polarization curve, open circuit potential, Mott-Schottky curve and immersion test.

## 2. EXPERIMENTAL

### 2.1. Specimen and solution

The test samples were cut from the hot-rolled plates of X65 and X80 pipeline steel. The chemical composition of X80 steel is (wt. %): C 0.070, Si 0.216, Mn 1.80, P 0.0137, S 0.0009, Mo 0.182, Cr 0.266, Cu 0.221, Ni 0.168, Nb 0.105, Al 0.026, Ti 0.013, V 0.001, N 0.003 and Fe balance. And the chemical composition of X65 steel is (wt. %): C 0.08, Si 0.22, Mn 1.62, P 0.011, S 0.001, Ni 0.02, Cr 0.02, Nb 0.04, Mo 0.004, V 0.02 and Fe balance. The microstructure of the two steels was characterized by a Quanta 250 scanning electron microscope (SEM).

In the lab,  $\text{Na}_2\text{CO}_3/\text{NaHCO}_3$  solution was usually used to investigate the corrosion behavior of buried pipelines operated in alkaline soil environment. In this paper, 0.3 M  $\text{Na}_2\text{CO}_3$  + 1 M  $\text{NaHCO}_3$  was adopted to study the corrosion behavior of X65 and X80 steels with AC application. The pH of the solution was about 9.32. The temperature of all tests was a constant temperature of 25°C.

### 2.2. Electrochemical tests

Different steel samples were coated with an epoxy, leaving an exposure area of 10 mm × 10 mm as the working surface. Before the test, the electrode was ground to 2000 grit emery paper, rinsed in distilled water and alcohol, and finally by air drying. Electrochemical tests were performed through PARSTAT2273 electrochemical workstation using a three-electrode cell system, where the two steel specimen was used as working electrode, a saturated calomel electrode(SCE) as reference electrode, and a platinum plate as counter electrode. The schematic diagram of the experimental set-up for studies of AC corrosion was in accord with our previous researches[12-13]. The sinusoidal AC signal with a frequency of 50 Hz was applied between the working electrode and graphite electrode. The AC current was root-mean-square value, and measured with a clamp meter.

Electrochemical measurements include potentiodynamic polarization curve, open circuit potential and Mott-Schottky curve. Prior to test, the specimen was soaked in the solution for 30 min to

reach a steady-state. Potentiodynamic polarization curves were tested at a potential scan rate of 0.5 mV/s, and the potential range was -1.0~1.2V (vs.SCE). During the test, AC with different current density (0, 30, 100 A/m<sup>2</sup>) was imposed to the working electrode. In addition, open circuit potential curves of the steels with AC current of 100 A/m<sup>2</sup> were measured for 30 min.

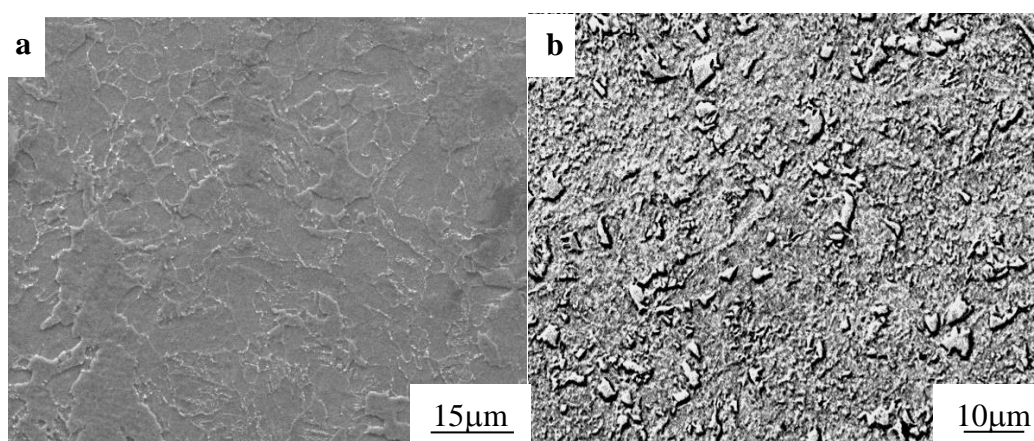
In order to investigate the different damage effect of AC on the passive films formed on the surface of the two steels, the Mott-Schottky curve was measured. This experiment design was described as followed. Firstly, using the potentiostatic passivation method to form a passive film on the surface of steel by DC circuit, then the specimen with the formed film interfered at AC current density of 100A/m<sup>2</sup> for 0.5 h by imposed AC circuit. Sequentially, AC current was removed. Finally the Mott-Schottky curve was measured via the electrochemical workstation. The passive film was anodically grown on the steels at an applied potential of 0.7 V (vs.SCE) for 2 h. The Mott-Schottky curve was conducted at a fixed frequency of 1kHz during a 50 mV/step in the potential range from -0.5 to 1.2 V (vs. SCE).

### 2.3. Immersion test

In this test, the samples were the same as those used in electrochemical test, and the superimposed AC circuit in the schematic diagram[12-13] was used. Before the test, the specimens were grinded, polished, and cleaned, then dried and weighed. The test was carried out for 72 h, with a 50 Hz sinusoidal signal with the AC current density ( $i_{AC}$ ) of 100 A/m<sup>2</sup> applied between the sample and graphite electrode. After the test, the corrosion product on the surface of steel specimen was removed thoroughly. Subsequently, the specimens were rinsed, air dried, and weighed carefully, and finally the corrosion rates of the two steels were calculated based on the weight-loss. The surface corrosion morphologies of the steels under AC interference were observed via SEM.

## 3. RESULTS

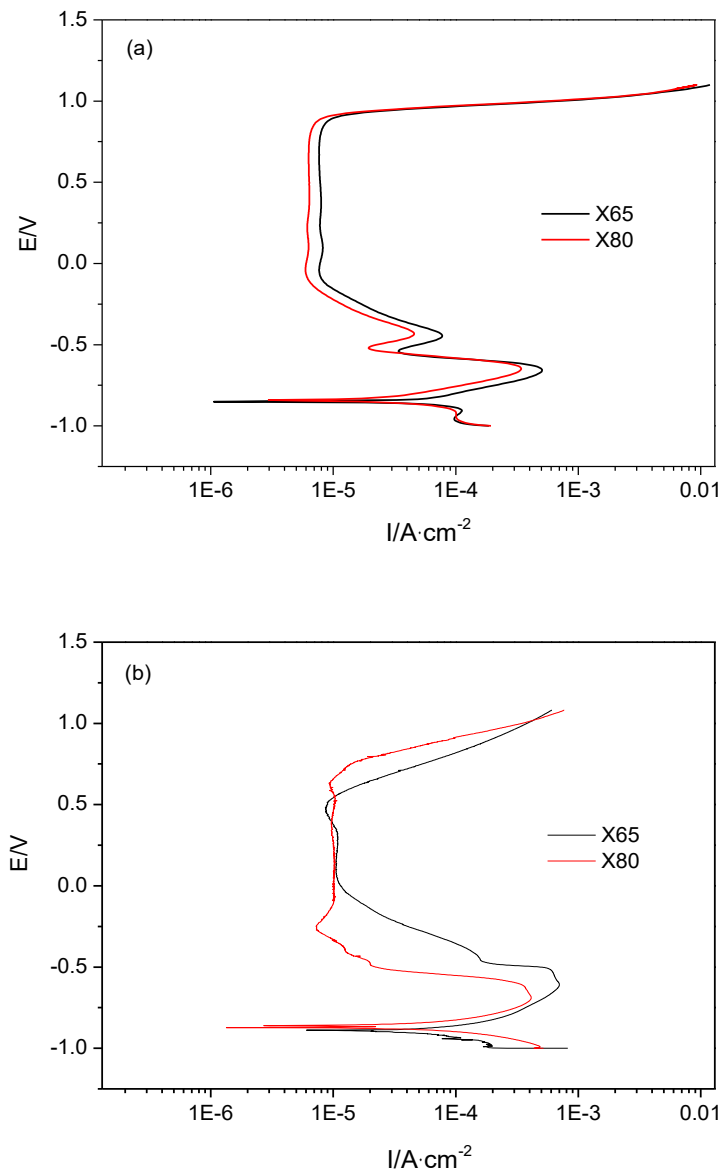
### 3.1 Microstructure observation



**Figure 1.** Microstructure of (a) X65 and (b) X80 steels

Fig.1 shows the microstructure of X65 and X80 steels. As seen in Fig.1a, the microstructure of X65 steel consists of large sized polygonal ferrite (PF) and pearlite (P). Fig.1b exhibits X80 steel is composed of acicular ferrite (AF), a small amount of polygonal ferrite (PF), and a certain number of granular bainites (GB). Compared with X65 steel, the grain of X80 steel is fine, and the grain boundary is discontinuous.

3.2. Electrochemical measurement



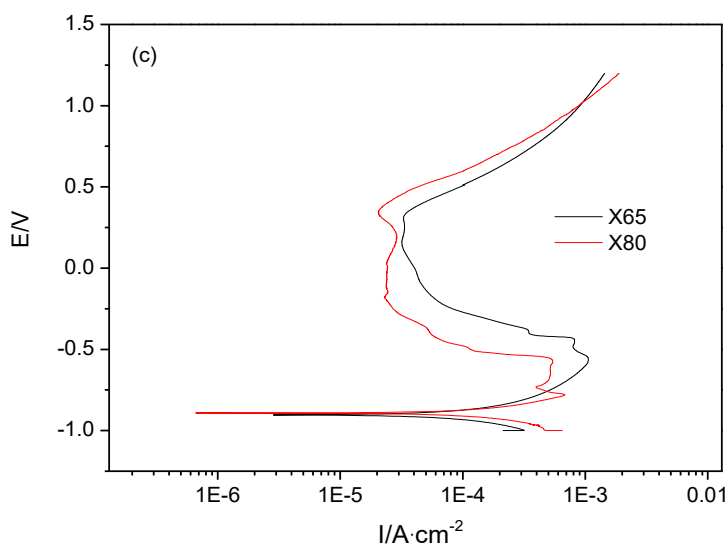


**Figure 2.** polarization curves of X65 and X80 steels at various AC current densities: (a) 0 A/m<sup>2</sup>, (b) 30 A/m<sup>2</sup>, (c) 100 A/m<sup>2</sup>

Fig.2 shows the polarization curves of X65 and X80 steels at various AC current densities. With AC application, the passivation area narrows, the critical pitting potential shifts negatively and the passive current density increases. The variation of anodic polarization curve indicates that AC could significantly reduce the passivity of the steels.

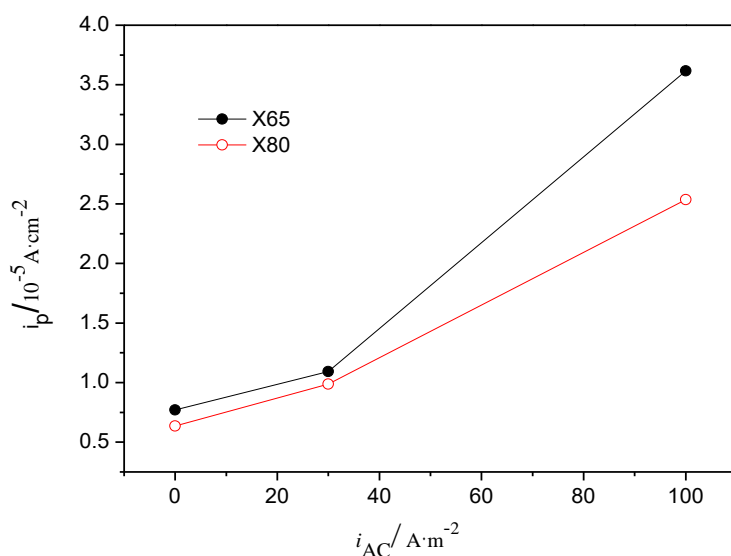


**Figure 3.** Passive current density of X65 and X80 steels at various AC current densities

Fig.3 displays the passive current densities ( $i_p$ ) of X65 and X80 steels at various AC current densities. The  $i_p$  of the two steels increases with the increase of AC current density ( $i_{AC}$ ). At the absence of AC or low  $i_{AC}$ ,  $i_p$  of the two steels are nearly equal, and X65 steel has a slightly greater  $i_p$  value. When  $i_{AC}$  increases up to 100A/m<sup>2</sup>, the  $i_p$  of X80 steel is far lower than that of X65 steel. This demonstrates that AC interference increases the instability of passive film formed on the steels, and the

film on X65 steel has a worse stability, with a larger corrosion rate. Moreover, Fig.2 exhibits that AC causes an obvious narrowing of passive region and relative large amplification negative shift of critical pitting potential, especially for X65 steel. This implies that AC could increase the pit corrosion susceptibility. Therefore, AC could increase instability of the passive film, interfere the formation of passive film, and AC current with high  $i_{AC}$  generates a more damage to the film.

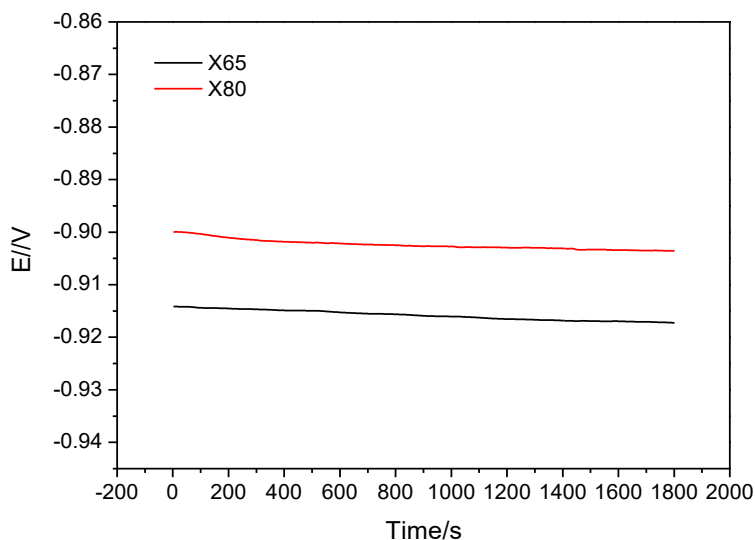


**Figure 4.** Open circuit potential of X65 and X80 steels at AC current density of 100A/m<sup>2</sup>

Fig. 4 shows the open circuit potential of X65 and X80 steels under AC application. It clearly displays that the corrosion potential of X65 steel at AC current density of 100A/m<sup>2</sup> is more negative than that of X80 steel. This indicates that X65 steel under AC interference has a higher electrochemical activity, that is, a larger corrosion tendency.

Known from the result of polarization curve, AC interference could reduce the stability of passive film on the steel surface. In order to further investigate the internal influence mechanism, the effect of superimposed AC on the semiconducting properties of passive films of X65 and X80 steels was studied by Mott-Schottky curve test. The application of the test to passive film is based on the existence of a depletion region within the passive film producing a space charge capacitance (C). The relationship between the capacitance and the applied potential is described by the Mott-schottky equation, which exhibits the applied potential dependence of the capacitance C for a semi-conductor junction [16-17] as:

$$C^{-2} = \pm \frac{2}{e\epsilon\epsilon_0 N} \left( E - E_{FB} - \frac{\kappa T}{e} \right) \quad (1)$$

where the negative sign (-) is for a p-type semiconductor and the positive sign (+) for n-type conductivity,  $e$  is the electron charge ( $1.602189 \times 10^{-19}$  C),  $N$  is the donor density ( $N_D$ ) for n-type or the acceptor density ( $N_A$ ) for p-type semiconductor.  $\epsilon_0$  is the vacuum permittivity ( $8.854 \times 10^{-14}$  F/cm),  $\epsilon$  is the relative permittivity (dielectric constant) of the passive film at room temperature, in this paper, the  $\epsilon$  is 15.6 [18-19].  $k$  is the Boltzmann's constant ( $1.38 \times 10^{-23}$  J/K),  $T$  is the Kelvin temperature, and  $\kappa T/e$  is about 25 mV at room temperature.  $E$  is the applied electrode potential and  $E_{FB}$  is the flat band

potential. The semiconductor type and defect concentration ( $N_D$  or  $N_A$ ) can be determined from the linear segment in a Mott-Schottky plot ( $C^2-E$ )[20].

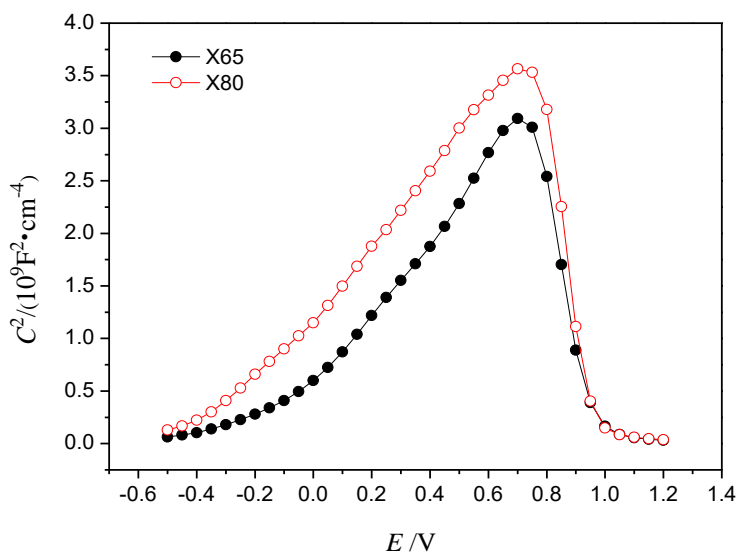


**Figure 5.** Mott-schottky curves of passive film of X65 and X80 steels at AC current density of  $100A/m^2$

Before the test, the passive films were formed on the surface of X65 and X80 steel specimens by the potentiostatic polarization method. Then the steel electrodes covered with passive films were interfered at  $i_{AC}$  of  $100A/m^2$  for 0.5 h, subsequently the Mott-Schottky curves of the two steels were measured. As displayed in Fig.5, the linear segment with positive slopes in the curves can be observed at the potential range from -0.6 to 0.6V (vs.SCE), suggesting that n-type semiconductor behavior [21] for the passive film of the two steels under AC interference.

According to the equation(2), the slopes of the linear segment of the curves give the donor density  $N_D$ , from the equation:

$$N_D = \frac{2}{m e \epsilon \epsilon_0} \tag{2}$$

where  $m$  is the slope of the linear segment in the Mott-Schottky curves,  $e$  is the electron charge,  $\epsilon$  is the relative permittivity (dielectric constant) of the passive film at ambient temperature, and  $\epsilon_0$  is the vacuum permittivity.

The calculated donor densities ( $N_D$ ) of the passive films of X65 and X80 steels are  $3.62 \times 10^{21} cm^{-3}$ ,  $2.75 \times 10^{21} cm^{-3}$  respectively. This indicates that the film of X65 steel under AC interference has a greater amount of point defects than that of X80 steel, and the inner structure of the film is more disordered[22-23]. Thus, the film of X65 steel with application of imposed AC exhibits a worse stability. Due to this, the film of X65 steel has a smaller charge transfer resistance, resulting in a greater corrosion rate.

According to the below equation (3), the space charge layer thickness [21]  $L$  can be obtained.

$$L = \left( \frac{2 \epsilon \epsilon_0}{e N_D} \right) \left( E - E_{FB} - \frac{\kappa T}{e} \right)^{\frac{1}{2}} \tag{3}$$

where  $N_D$  is the donor density, and others parameters value are in accordance with the equation (1).

Because X65 steel under AC interference has a larger  $N_D$  value, so the steel possesses a thinner space charge layer thickness  $L$ , i.e., the thickness of passive film. This means that the film of X65 steel with AC application is more unstable, and the film easily ruptures, which is beneficial to the occurrence of pit corrosion. Combined with the result of polarization curve, the influence of AC on passive film of different steels causes a difference in the corrosion resistance.

### 3.3. Immersion test

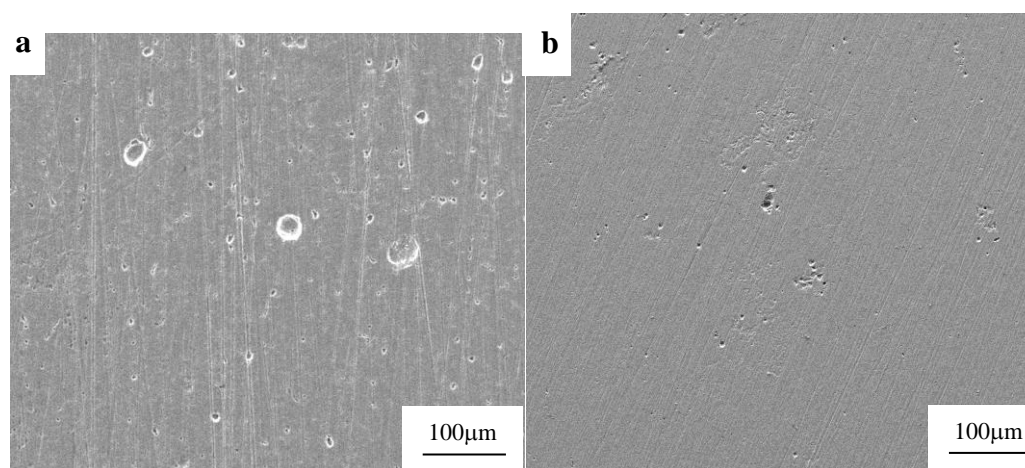


**Figure 6.** Corrosion morphologies of X65 and X80 steels at AC current density of  $100\text{A/m}^2$  after removing the corrosion product: (a)X65 steel, (b) X80 steel

Fig.6 exhibits the corrosion morphologies of X65 and X80 steels at AC current density of  $100\text{A/m}^2$  after removing the corrosion product. Fig.6a displays a more severe localized corrosion on the surface of X65 steel under AC interference, compared with that of X80 steel. A certain number of small-sized pits and a small amount of relative large-sized pits are distributed on X65 steel surface. By contrast, X80 steel has a slighter corrosion status, with a low intensity pits. Consequently, X65 steel has a higher corrosion rate than X80 steel, and the corrosion rates of the two steels are  $0.176\text{ mm/a}$ ,  $0.122\text{mm/a}$  respectively. Moreover, X65 steel has a larger susceptibility to pit, which is in accord with the polarization curve analysis.

Based on the above analysis, X80 steel under AC interference has a better corrosion resistance than X65 steel. This may be related with the different microstructure. Fig.1a exhibits that the microstructure of X65 steel consists of large sized polygonal ferrite (PF) and pearlite (P). Due to the potential difference between the two phases, the ferrite and pearlite can generate a great amount of galvanic-type corrosion cells, which would facilitate the corrosion of X65 steel. Furthermore, pearlite is a eutectoid compound, which consists of two composition phases of ferritic and cementite. Likewise, the potential difference between the two phases would form numerous micro-galvanic corrosion cells [24-25] and accelerate the corrosion occurrence. Combined with the corrosion feature (Fig.6a), X65

steel under AC interference has a worse corrosion resistance. Fig.1b reveals that X80 steel is composed of acicular ferrite (AF), a small amount of polygonal ferrite (PF), and a certain number of granular bainites (GB), which is analogous to a single phase microstructure, so the micro-galvanic corrosion cells significantly decrease. Therefore, X80 steel shows a better corrosion resistance.

#### 4. CONCLUSIONS

AC could significantly reduce the passivity of the steels, interfere with the formation of passive film, increase the instability of passive film formed on the steel, and AC with high  $i_{AC}$  generates a more damage to the film. The film on X65 steel has a worse stability, with a larger corrosion rate. Under AC interference, X65 steel has a worse corrosion resistance, with a more severe localized corrosion. While X80 steel exhibits a better corrosion resistance, with a slighter corrosion status. The microstructure consisting of ferrite and pearlite is more susceptibility to AC corrosion.

#### ACKNOWLEDGEMENTS

This work was support by the National Natural Science Foundation of China (No. 51501164), the Natural Science Foundation of Zhejiang province (No. LY18E010004), the Project Funded by China Postdoctoral Science Foundation (No.2017M621974), and the National R&D Infrastructure and Facility Development Program of China (No. 2005DKA10400).

#### References

1. Y. Hosokawa, F. Kajiyama and T. Fukuoka, *Corrosion*, 60(2004)408.
2. S.B. Lalvani and G. Zhang, *Corros. Sci.*, 37(1995)1567.
3. S.B. Lalvani and G. Zhang, *Corros. Sci.*, 37(1995)1583.
4. Y.B. Guo, H.Tan, D.G. Wang and T. Meng, *Anti-Corros. Method.M.*, 64(2017)599.
5. H.R. Hanson and J. Smart, AC Corrosion on a Pipeline Located in an HVAC Utility Corridor, CORROSION 2004, Houston, America, 2004, 209.
6. L.V. Nielsen, K.V. Nielsen, B. Baumgarten, H. Breuning-Madsen, P. Cohn and H. Rosenberg, AC-Induced Corrosion in Pipelines: Detection, Characterisation, and Mitigation, CORROSION 2004, Houston, America, 2004, 211.
7. R.G. Wakelin and C. Sheldon, Investigation and Mitigation of AC Corrosion on a 300mm Diameter Natural Gas Pipeline, CORROSION 2004, Houston, America, 2004, 205.
8. L.Y. Xu, X. Su, Z.X. Yin, Y.H.T ang and Y.F. Cheng, *Corros. Sci.*, 61(2012)215.
9. A.Q. Fu and Y.F. Cheng, *Corros. Sci.*, 52(2010)612.
10. H. Song, Y.G. Kim, S.M. Lee, and Y.T. Kho, Competition of AC and DC Current in AC Corrosion under Cathodic Protection, CORROSION 2002, Houston, America, 2002, 117.
11. D. Kuang and Y.F. Cheng, *Corros. Sci.*, 85(2014)304.
12. M.Z hu, C.W. Du, X.G. Li, Z.Y. Liu, H. Li and D.W. Zhang, *Corros. Sci.*, 87(2014)224.
13. M. Zhu, C.W. Du, X.G. Li, Z.Y. Liu, S.R. Wang, J.K. Li and D.W. Zhang, *Electrochim. Acta*, 117(2014) 351.
14. L.W. Wang, L.J. Cheng, J.R. Li, Z.F. Zhu, S.W. Bai and Z.Y. Cui, *Materials*, 11(2018)465.
15. H.X. Wan, D.D. Song, Z.Y. Liu, C.W. Du, Z.P. Zeng, X.J. Yang and X.G. Li, *J.Nat. Gas Sci. Eng.*, 38(2017)458.

16. V. A. Alves and C.M.A. Brett, *Electrochim. Acta*, 47(2002)2081.
17. J. Sikora, E. Sikora and D.D. Macdonald, *Electrochim. Acta*, 45(2000)1875.
18. P. Schmuki and H. Bohni, *Electrochim. Acta*, 40 (1995)775.
19. W. S. Li and J. L. Luo, *Corros. Sci.*, 44(2002)1695.
20. A. Goossens, M. Vazquez and D.D. Macdonald, *Electrochim. Acta*, 41(1996)35.
21. S. Ningshen, U. Kamachimudali, V. Mittal and H. Khatak, *Corros. Sci.*, 49(2007)481.
22. H. Luo, C.F. Dong, X.G. Li and K. Xiao, *Electrochim. Acta*, 64(2012)211.
23. H. Luo, C.F. Dong, K. Xiao and X.G. Li, *Appl. Surf. Sci.*, 258(2011)631.
24. D. Clover, B. Kinsella, B. Pejic and R.De Marco, *J. Appl. Electrochem.*, 35(2005)139.
25. H.J. Cleary and N.D. Greene, *Corros. Sci.*, 9(1969)3.

© 2018 The Authors. Published by ESG ([www.electrochemsci.org](http://www.electrochemsci.org)). This article is an open access article distributed under the terms and conditions of the Creative Commons Attribution license (<http://creativecommons.org/licenses/by/4.0/>).